A transferred recurrent neural network for battery calendar health prognostics of energy-transportation systems

Liu, K., Peng, Q., Sun, H., Fei, M., Ma, H., & Hu, T. (2022). A transferred recurrent neural network for battery calendar health prognostics of energy-transportation systems. *IEEE Transactions on Industrial Informatics*, *18*(11), 8172-8181. https://doi.org/10.1109/TII.2022.3145573

Published in:
IEEE Transactions on Industrial Informatics

Document Version:
Publisher's PDF, also known as Version of record

Queen's University Belfast - Research Portal:
Link to publication record in Queen's University Belfast Research Portal

A Transferred Recurrent Neural Network for Battery Calendar Health Prognostics of Energy-Transportation Systems

Kailong Liu, *Member, IEEE*, Qiao Peng, Hongbin Sun, *Fellow, IEEE*, Minrui Fei, Huimin Ma, *Senior Member, IEEE*, and Tianyu Hu, *Member, IEEE*

***Abstract*—Battery-based energy storage system is a key component to achieve low carbon industrial and social economy, where battery health status plays a vital role in determining the safety and reliability of energy-transportation nexus. This paper proposes a transferred recurrent neural network (RNN)-based framework to achieve efficient calendar capacity prognostics under both witnessed and unwitnessed storage conditions. Specifically, this transferred RNN framework contains a base model part and a transfer model part. The base model is first trained by using the easily-collected and time-saving accelerated ageing dataset from high temperature and SOC cases. Then the transfer part is tuned by using only a small portion of starting capacity data from unwitnessed condition of interest. The developed framework is evaluated under a well-rounded ageing dataset with three different storage SOCs (20%, 50%, and 90%) and temperatures (10℃, 25℃, and 45℃). Experimental results demonstrate that the derived transferred RNN framework is capable of providing satisfactory calendar capacity health prognostics under different storage cases. A model structure with the impact factor terms of SOC and temperature outperforms other counterparts especially for the unwitnessed conditions. The proposed framework could assist engineers to significantly reduce battery ageing experiment burden and is also promising to capture future capacity information for battery health and life-cycle cost analysis of energy-transportation applications.**

***Index Terms*—Energy and transportation informatics; Health and life-cycle analysis; Battery calendar capacity; Transfer learning; Data-science.**

Manuscript received Aug 24, 2021; revised Nov 04, 2021, Dec 09 2021; accepted Jan 09, 2022. This work was supported by HVM Catapult project under 160080 CORE, the National Natural Science Foundation of China (No. U20B2062, 62172036), and the Key Project of Science and Technology Commission of Shanghai Municipality (No. 19500712300,19510750300). (*Corresponding authors: Tianyu Hu, and Huimin Ma*).

K. Liu is with the Warwick Manufacturing Group, The University of Warwick, Coventry, CV4 7AL, United Kingdom (Email: kliu02@qub.ac.uk, Kailong.Liu@warwick.ac.uk).

Q. Peng is with the Queen's University Belfast, BT7 1NN, United Kingdom (Email: qpeng01@qub.ac.uk).

H. Sun is with the Department of Electrical Engineering, State Key Laboratory of Power Systems, Tsinghua University, Beijing, China. (Email: shb@tsinghua.edu.cn).

M. Fei is with the School of Mechatronic Engineering and Automation, Shanghai University, Shanghai 200444, China (Email: mrfei@staff.shu.edu.cn).

H. Ma and T. Hu are with the School of Computer and Communication Engineering, University of Science and Technology Beijing, Beijing, China. (Email: tianyu@ustb.edu.cn, mumpub@ustb.edu.cn)

I. INTRODUCTION

Due to the superiority of high energy density and low self-discharging rate, lithium-ion (Li-ion) battery has been widely adopted in many energy-based transportation applications such as electric vehicles (EVs) to achieve low carbon industrial and social economy [1]. However, the reliability and performance of battery-based energy storage system would be inevitably reduced during its service life [2]. After manufacturing, a battery would be operated with two main modes: calendaring and cycling. Considering more than 75% of battery operational time is spent under the storage cases for most EV applications, it is vital to design suitable methods for calendar health prognostics of battery-based energy storage system [3,4].

In the calendaring mode of Li-ion battery, the capacity fading rate is significantly affected by several impact factors including its storage state-of-charge (SOC) and temperature levels [5]. As a complicated process with highly nonlinear and strongly coupled relations, developing effective prognostic model to capture and predict battery capacity degradation dynamics under various storage conditions while taking into account both SOC and temperature's effects is significantly important for improving energy-transportation nexus. Nowadays, the mainstream approaches to predict battery calendar health dynamics contain two groups: specific model-based approach and data-driven model-based approach.

For the specific model-based approach, several elements that could reflect the calendar degradation mechanisms are coupled within a model to reflect battery health degradation behaviors. For example, through coupling a side reaction exchange current item, an improved battery electrochemical model is proposed in [6] to capture calendar capacity dynamics under various SOCs but constant temperature. Besides, based upon some specific knowledge forms such as the Eyring acceleration or Arrenhius law equations, semi-empirical models have been widely used as another specific model type to describe battery health degradation behavior with impact factors. For instance, De Hoog et al. [7] proposes a semi-empirical model for battery calendar service life prediction with the consideration of battery storage conditions. In [8], after considering cell formation effects, a semi-empirical model is designed to predict battery

future calendar degradation status.

On the other hand, with the rapid development of data science and informatics methodology, data-driven model-based approach has become another popular solution for battery health management [9,10]. After collecting available battery ageing data, different data-driven models through using various machine learning (ML) technologies such as support vector machine [11], Gaussian process regression (GPR) [12], and neural network (NN) [13,14] have been successfully designed for battery health prognostics. For example, Ma et al. [15] propose a hybrid NN to effectively predict the battery degradation trajectories under cyclic conditions. After deriving a data-driven Brownian motion model, Dong et al. [16] achieves the effective degradation modelling and remaining useful life (RUL) prediction of Li-ion battery. Among these researches, on the one hand, according to the related review publication [17], several ML methods appear to be promising for performing battery capacity health prognostics with time-series nature. For example, through augmenting the recurrent links to the hidden layers, recurrent neural network (RNN) becomes a powerful solution for extracting and updating correlation of sequential battery capacity ageing data [18,19]. Recently, according to the extracted time-varying current and voltage, an RNN-based model is designed in [20] to obtain reliable information of interested battery capacities. Through deriving an RNN-based framework, Zhang et al. [21] captured the long-term degradation trend of Li-ion battery. In [22], after combining the benefits of both RNN and GPR, a hybrid data-driven approach is proposed to predict battery future capacities and RUL with uncertainty quantification during cyclic mode. On the other hand, although reasonable capacity predictions could be achieved for effective battery health management through designing suitable data-driven model, some limitations still need to be further improved as: 1) most researches mainly focus on battery capacity prediction under the same constant conditions, ignoring the effects of different temperatures and SOC levels. According to [23], high storage temperature and SOC would accelerate the increasing rate of solid electrolyte interface (SEI) on the battery's anode, further speeding up battery calendar ageing process. Such models are difficult to capture battery health behaviors under different storage conditions. 2) To ensure a data-driven model could effectively study enough underlying information of battery ageing under various cases, a mass of experimental ageing data from these cases are generally required in the training phase. In general, the generation of battery ageing data requires large experimental burden and long experimental time (several months to years). Numerous researches mainly focus on exploring the extrapolated prediction performance of data-driven models under the same conditions as the training data. In this context, engineers are very interested in discovering a suitable way that the data-driven models are just trained based on some easily-collected ageing data, while the trained model can be conveniently transferred to perform future capacity prognostics with satisfactory prediction performance under other unwitnessed conditions [24]. Therefore, how to develop battery health prognostic model with limited training data and achieve accurate battery capacity degradation predictions particular for unwitnessed cases is still a key but challenging issue.

Considering the aforementioned limitations and challenges, an efficient data-driven framework through devising the transferred RNN model is proposed in this study for calendar health prognostics of Li-ion battery under various SOC and temperature cases. Several main contributions are summarized as: 1) to reduce training cost and required battery ageing data, a novel RNN-based framework with the transfer concept is proposed. Specifically, this transferred RNN framework contains a base model part and a transfer model part. The base model part is trained by using the accelerated ageing dataset while the transfer model part is adjusted by only adopting a few starting data from unwitnessed storage cases. 2) two battery ageing prognostic model structures are derived based on the systematical analysis of impact factors of battery calendar ageing: i) by involving the information of current capacity value and future time period as inputs, Model 1 is able to predict future capacity points with a simple structure; ii) by adding another two additional input terms of battery storage SOC and temperature, Model 2 is capable of considering the effects of these two key impact factors during future capacity prognostics. 3) the performance of proposed transferred RNN-based data-driven framework is explored and evaluated based on a well-rounded battery calendar ageing dataset containing 27 capacity series under nine different storage cases. Obviously, after training by the accelerated ageing data and adjusting by a portion of starting unwitnessed ageing data, the proposed framework is able to provide satisfactory battery calendar degradation prognostics for both witnessed and unwitnessed cases. Through considering the effects of SOC and temperature, Model 2 outperforms other counterparts in most prediction cases. Due to data-driven and transfer nature, the proposed framework can be utilized to predict battery future calendar capacity points under various storage cases when a few starting ageing data are available.

The remainder of this paper is organized as follows. Section II specifies the calendar ageing experiment and related battery ageing datasets. Then the fundamental of RNN is first described in Section III, followed by the detailed description of derived transferred RNN and related framework to perform battery capacity degradation prognostics. Besides, two powerful battery ageing prognostic models with different input terms, and the corresponding evaluation metrics are also given. Section IV presents the in-depth analyses of proposed transferred RNN-based framework for future battery calendar capacity predictions via three case studies. Finally, Section V concludes this work.

II. CALENDAR HEALTH DEGRADATION EXPERIMENT

To generate suitable battery dataset for model development and evaluation, battery calendar health ageing experiments under different storage cases are carried out based on a battery health experimental platform, as illustrated in Fig. 1. Specifically, this platform can be divided into three parts: a MACCOR 400 battery charger to control the storage SOCs of batteries, a

thermal chamber to maintain batteries with preset environmental temperature, and a PC to monitor and manage battery calendar ageing data collected from experiments. Here the adopted battery has a 2.9Ah nominal capacity with the positive electrode of nickel cobalt aluminum oxides (NCA) and negative electrode of graphite. Its lower and upper cut-off voltages are 2.5V and 4.2V respectively. The suggested operational temperature of this battery is 10℃ to 45℃. In this study, 27 battery calendar capacity degradation experiments under nine various storage cases (three SOCs and three temperature levels) are carried out with the detailed information shown in Table I. To be specific, the storage SOC cases are 20%, 50%, and 90%, while the storage temperature levels are 10℃, 25℃, and 45℃, formulating a 3×3 battery storage matrix. The battery calendar capacity ageing data for each experiment are collected with a length of 17 measures every 30 days (720 hours). A periodic check-up is performed every 720 hours to measure the reference capacities of the batteries in storage mode. Specifically, for each check-up, the temperature chamber would be first set to 25℃. Then a constant current-constant voltage (CCCV) profile is adopted to fully charge each battery cell. After resting for 3 hours, a CC profile with 1/3C current will be adopted to fully discharge each cell to its lower cut-off voltage (2.5V). Then each reference capacity point is calculated by summing all discharged currents based on the Ampere-hour-integral approach. Afterwards, to calibrate cell SOC, the CCCV profile will be adopted to fully recharge these cells. Then after another resting period of 3 hours, each cell will be discharged to its specific SOC setpoint based on the well-controlled coulomb counting approach. Besides, the temperature chamber would be reset to the specific storage temperature value again. For each storage condition, three cells are used to generate three capacity series for guaranteeing the repeatability of this storage case.

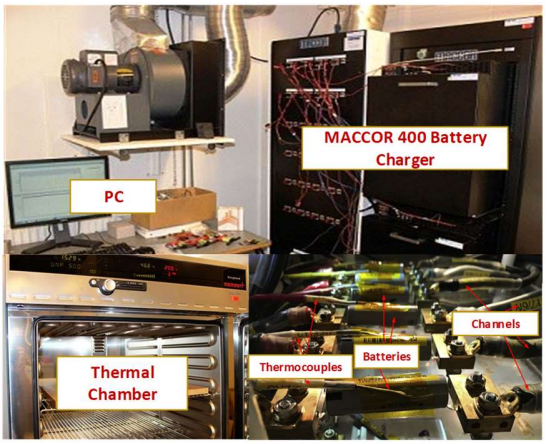

Fig. 1. Battery calendar health experimental platform.

According to these calendar ageing experiments, 27 battery cell capacity series covering 11520 hours are obtained in total. Several capacity series present an initial fast capacity degradation followed by a more linear reduction. This is mainly due to the fact that anode electrode presents excess area compared with the cathode electrode, which is described as anode overhang in literatures [25]. For the real battery

TABLE I
BATTERY CALENDAR AGEING DATASET

		Storage temperature					
		10℃	25℃		45℃		
SOC	20%	Test5(B)	Test1(B)		Test2(B)		
	50%	Test3(B)	Series 1	Test1 (A)	Series 3	Test2 (A)	
			Series 2		Series 4		
			Vali1		Vali2		
	90%	Test4(B)	Series 5	Test3 (A)	Series 7	Test4 (A)	
			Series 6		Series 8		
			Vali3		Vali4		

applications, it should be known that higher SOC and temperature levels would cause battery to degrade more rapidly. This is mainly due to that the high storage SOC and temperature would accelerate the increasing rate of solid SEI on battery's anode, further speeding up battery calendar ageing process [23]. That is, during the same storage time period, capacity series under high SOCs and temperatures would present larger degradation ratio [26]. In this context, it is meaningful to derive a reliable battery calendar prognostic model only using this type of accelerated battery ageing data, while this model is also able to generalize well for other unwitnessed cases. One obvious benefit of this is that the experiment time and cost to generate suitable data for model training could be significantly reduced. To achieve this, the whole battery calendar ageing dataset is divided into four parts with various colors in Table I. Specifically, training dataset consists of these capacity series (Series 1, 2,…, 8) in blue from four accelerated battery storage cases, whose timestamp is no longer than 7920 hours. Then the dataset (Vali1,2,…,4) to validate the performance of model training contains four capacity series in yellow from the same storage cases with the timestamp within 7920 hours. To test the performance of the battery calendar ageing prognostic model, two test sets after using the mean values of three cells' capacities under the same storage condition are formulated in this study: the test set A beyond 7920 hours (four series in green) from accelerated battery storage cases is used to evaluate the model's exploration ability under the witnessed conditions, while the test set B (five series in purple) from another battery storage cases is adopted to evaluate model's generalization ability under the unwitnessed conditions.

III. METHODOLOGY

This section first describes the fundamental of RNN, followed by the elaboration of derived transferred RNN and related framework. Then two different ageing prognostics models within the framework to predict battery future calendar capacities under both witnessed and unwitnessed storage cases are presented. Finally, several typical evaluation metrics are given for quantifying the performance of model prognostics.

A. Recurrent neural network

Due to the involved augment recurrent link to different layers, RNN belongs to a classical neural network with the abilities of extracting as well as updating correlation particular for sequential data. In order to alleviate the issues of gradient vanishing, a typical long short-term memory (LSTM) structure

is generally integrated with the RNN through embedding three types of gates (input, forget and output) [27]. In this context, key information from inputs can be stored and updated through operating these gates, further ensuring the related information could be kept over a long period without causing gradient vanishing issue.

As shown in Fig. 2, a classical LSTM-based RNN model generally consists three gate parts. Their states are controlled by a in_k (the input at the current time sample k) as well as a out_{k-1} (the output at the previous time sample $k-1$) by using the sigmoidal units. Here the input gate would decide if a new state information $\widetilde{sta}_k$ could be received by the RNN. The forget gate will decide which previous state $\widetilde{sta}_{k-1}$ from hidden layers should be forgot, while the output gate would be responsible for determining which information predicted by the RNN should be outputted as out_k. Specifically, detailed processes of each gate within RNN are:

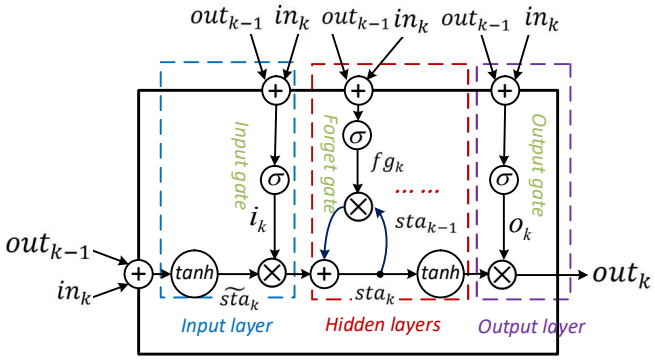

Fig. 2. RNN model with LSTM structure.

Process 1: For the input gate part, the states of $\widetilde{sta}_k$ as well as input gate i_k would be updated as:

$$\begin{cases} \widetilde{sta}_k = tanh(A_s in_k + B_s out_{k-1} + c_s) \\ i_k = \sigma(A_i in_k + B_i out_{k-1} + c_i) \end{cases} \quad (1)$$

Process 2: For the forget gate part, the state of forget gate fg_k as well as state sta_k would be updated as:

$$\begin{cases} fg_k = \sigma\left(A_f in_k + B_f out_{k-1} + c_f\right) \\ sta_k = i_k \otimes \widetilde{sta}_k + fg_k \otimes sta_{k-1} \end{cases} \quad (2)$$

Process 3: For the output gate part, the states of output gate o_k as well as output out_k would be updated as:

$$\begin{cases} o_k = \sigma(A_o in_k + B_o out_{k-1} + c_o) \\ out_k = o_k \otimes \tanh\left(sta_k\right) \end{cases} \quad (3)$$

where $\otimes$ represents the elementwise multiplication. σ and tanh stand for the sigmoid activation function and hyperbolic tangent activation function, respectively. A_* and B_* are their corresponding weight matrices. c_* is a vector to reflect their corresponding bias. For capacity prognostic applications, it should be known that more than one hidden layer can be used to increase the capture and mapping ability of RNN.

B. Designed transferred RNN

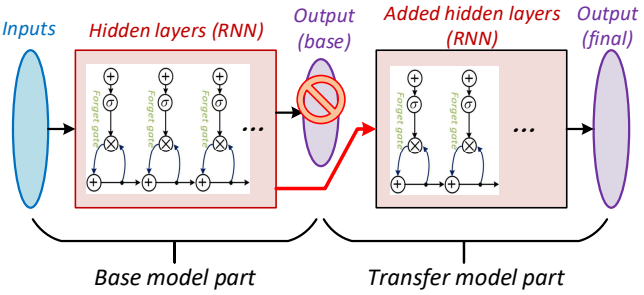

Fig. 3. Structure of derived transferred RNN.

As discussed in the previous section, a model that only uses the accelerated ageing dataset for training purpose but is capable of performing accurate battery calendar degradation prognostics is significantly meaningful, considering the huge experimental cost and time for generating available battery ageing data [17]. However, this would result in a big challenge for data-driven model-based approaches as the underfitting issue is easy to occur under the conditions that just a little information could be learned from limited training data [28]. According to the idea of transfer learning [29], to handle this challenge, a novel solution by designing an effective transferred RNN is derived in this study.

Fig. 3 illustrates the structure of designed transferred RNN. In comparison with the classical RNN structure shown in Fig. 2, the obvious difference is that the output layer of transferred RNN is modified with another added hidden layers, further leading the transferred RNN structure contains a base model part as well as a transfer model part. According to this structure, the base model part could be trained by using the dataset that easier to be obtained while the transfer model part could be adjusted by another dataset that is relatively difficult to be collected. Compared with the case of readjusting base RNN's parameters directly by just using a small portion of unwitnessed capacity data, the underlying mapping information studied in the base model part of our designed transferred RNN framework could be adopted as a guidance, further benefitting battery future long-term prediction performance under unwitnessed storage case.

Detailed framework of using this transferred RNN structure to learn the underlying ageing information from the accelerated ageing dataset and then perform reliable battery future capacity predictions under unwitnessed storage conditions is summarized in Fig. 4 with four key steps as follows:

Step 1. Base model part optimization: after preparing the accelerated ageing dataset under the storage cases of large SOCs (50%, 90%) and high temperatures (25℃, 45℃), eight related series (Series 1, 2,…, 8) are used to train the base model part of transferred RNN, while the dataset from four validation series (Vali1, 2,…, 4) is adopted to validate the performance of the trained base model.

Step 2. Capacity predictions for witnessed cases: for the extrapolated predictions under the witnessed cases (same storage conditions of training series), their future battery calendar capacity points could be predicted by using the well-trained base RNN model directly.

Step 3. Transfer model part optimization: for the extrapolated predictions of battery capacities under the unwitnessed storage conditions, after training base model

sufficiently, its output layer (red cross shown in Fig. 3) would be removed. Additional hidden layers and a new final output layer are then added just after the pre-determined hidden layers of the base model to formulate the transfer model part. Then this transfer model part would be adjusted by using only a small portion of capacity ageing dataset starting from an unwitnessed storage condition of interest. It should be known that during the optimization stage of the transfer model part, the base model part should be fixed without changing anything of its input and hidden layers.

Step 4. Capacity predictions for unwitnessed cases: after using a small portion of starting capacity ageing dataset to train transfer model part, the well-trained transferred RNN model is able to perform battery future calendar capacity predictions for this specific unwitnessed storage condition.

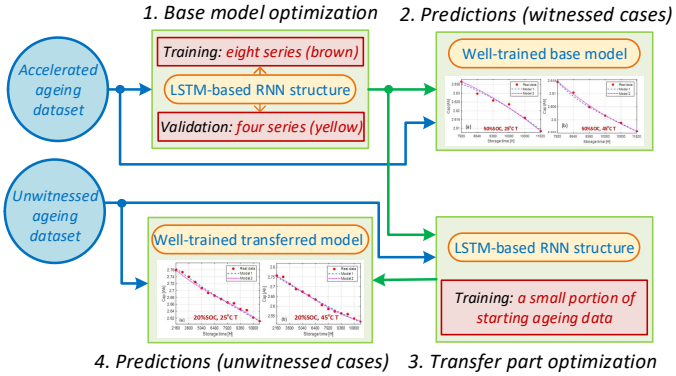

Fig. 4. Framework of deriving transferred RNN to predict future calendar capacity points for both witnessed and unwitnessed cases.

Based upon these steps, a transferred RNN-based framework could be established to predict battery future calendar capacity points from both witnessed and unwitnessed storage cases. Due to the involved transfer model part of this framework, the base model can be well trained by using accelerated battery ageing data, while only a few starting dataset from unwitnessed case of interest is required for model readjustment. Then the well-trained transferred RNN could provide effective battery future calendar capacity prognostics for this unwitnessed (lower temperature and SOC) case.

C. Ageing prognostics model

For battery calendar degradation prognostics, a proper model structure plays a vital role in affecting and determining the performance of battery future capacity prediction. In this study, based upon the transferred RNN framework as discussed in the previous subsection, two model structures are adopted, as illustrated in Fig. 5 and Fig. 6, respectively.

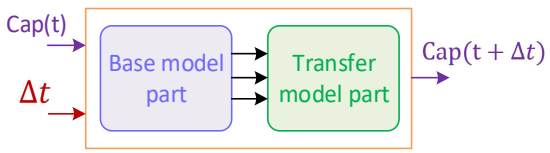

Fig. 5. Structure of battery ageing prognostics Model 1.

Supposing $\mathrm{Cap(t)}$ represents the battery capacity value at the current time sample t, Δt stands for the future time period of interest, then Model 1 has two input terms including $\mathrm{Cap(t)}$ and Δt , while its output is the corresponding battery future capacity value $\mathrm{Cap(t + \Delta t)}$ at time $\mathrm{t + \Delta t}$. For Model 2 as illustrated in Fig. 6, apart from the similar terms $\mathrm{Cap(t)}$ as well as Δt, another two terms SOC and T that reflect the storage SOC and temperature of interest are also used as the inputs of Model 2, while $\mathrm{Cap(t + \Delta t)}$ is adopted as its output as well. It should be known that by involving these two terms, the information of storage temperature and SOC for each calendar degradation case could be thus captured during the training process of Model 2, making it also able to reflect the underlying mapping among calendar capacity degradation and relevant storage cases. In this context, more information especially for the storage conditions of battery would be learned by Model 2.

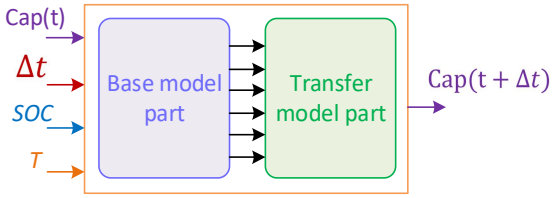

Fig. 6. Structure of battery ageing prognostics Model 2.

D. Evaluation metrics

To quantify and evaluate battery calendar degradation prognostics performance of designed models, several evaluation metrics are adopted in this study.

1) Mean absolute error (MAE): let N represents the total number of predicted future capacity points, $Ccal_i$ denotes the real battery capacity values, while $\widehat{Ccal_i}$ stands for the predicted capacity values from derived transferred RNN model, then the MAE to evaluate model's prognostic accuracy could be obtained by:

$$MAE = \frac{1}{N}\sum_{i=1}^{N}\left|Ccal_i - \widehat{Ccal_i}\right| \quad (4)$$

2) Root mean square error (RMSE): following the same definition, RMSE can be obtained to quantify the deviations between predicted calendar capacity points and real capacity points as:

$$RMSE = \sqrt{\frac{1}{N}\sum_{i=1}^{N}\left(Ccal_i - \widehat{Ccal_i}\right)^2} \quad (5)$$

3) R^2: let $\overline{Ccal}$ represents the mean point of all predicted battery calendar capacity points, R^2could be then obtained to quantify how closely the predicted future calendar capacity points get close to the real points as:

$$R^2 = 1 - \sum_{i=1}^{N}\left(Ccal_i - \widehat{Ccal_i}\right)^2 / \sum_{i=1}^{N}\left(Ccal_i - \overline{Ccal}\right)^2 \quad (6)$$

For our future battery calendar capacity prognostics cases, when the predicted calendar capacities match well with real capacity points, both MAE and RMSE become close to 0, while R^2 could get close to 1. According to these evaluation metrics, the prediction performance from derived transferred RNN models can be quantified and evaluated.

IV. Results and Discussions

This section in-depth analyses the performance of derived transferred RNN models for battery calendar degradation

prognostics via three case studies, with a special focus on the accuracy and generalization of proposed models. Here, all case studies are performed by using Matlab programming language in Matlab2020 with a 2.40 GHz Intel Pentium 4 CPU, while the related computational burdens are all within 20s. The derived transferred RNN models are trained by using the typical gradient descent-based optimization algorithm [30]. As each reference capacity point is measured with a storage period of 720 hours [H], the values of Δt in each calculation are set as the integer multiple values of 720 [H].

A. Case study for validation set

After using all capacity ageing data before 7920 hours from eight accelerated capacity series in blue to train the base model part, the predicted results from another four capacity series in yellow before 7920 hours from the same storage cases of SOCs (50%, 90%) and temperatures (25℃, 45℃) are utilized for validation purpose. The validation results and corresponding evaluation metrics from both Model 1 with a simple structure of two input terms (Cap(t) and Δt) and Model 2 with another two additional impact factor terms (SOC and T) are explored and compared, as illustrated in Fig. 7 and Table II, respectively.

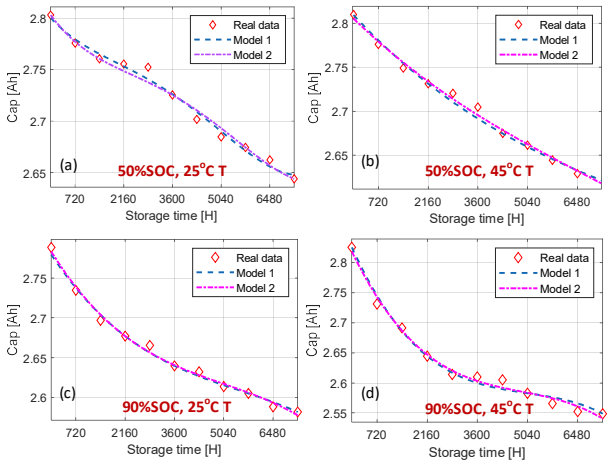

Fig. 7. Calendar validation results for cells under different storage cases: a) Vali 1 set, b) Vali 2 set, c) Vali 3 set, d) Vali 4 set.

TABLE II
EVALUATION METRICS FOR CASE STUDY OF VALIDATION SET

Vali set	Model 1			Model 2		
	MAE [Ah]	**RMSE [Ah]**	R^2	**MAE [Ah]**	**RSME [Ah]**	R^2
Vali 1	0.023	0.0076	0.98	0.024	0.0073	0.99
Vali 2	0.015	0.0054	0.99	0.011	0.0051	0.99
Vali 3	0.018	0.0058	0.99	0.017	0.0057	0.99
Vali 4	0.021	0.0063	0.98	0.020	0.0059	0.98

From Fig. 7, it can be seen that both Model 1 and Model 2 are able to capture the overall battery capacity degradation trends of validation set. Here Vali 2 owns the best validation results with 0.0054Ah RMSE for Model 1 and 0.0051Ah RMSE for Model 2. In contrast, Vali 1 achieves the largest MAEs of 0.023Ah for Model 1 and 0.024Ah for Model 2, which are obtained around 2880 hours. The RMSE values for Vali 1 also reach the largest ones, which are 40.7% and 43.1% larger than those of Vali 2. However, the R^2 values of these four sets (Vali 1, 2, 3, and 4) are all over 0.98, indicating that the satisfactory validation results could be achieved with accurate capacity prediction performance for both Model 1 and Model 2. In light of this, the base model part of the designed transferred RNN framework is capable of providing effective capacity degradation prognostics for the validation set under the same storage conditions of the training series.

B. Case study for test set A

Next, we focus on the evaluation of extrapolated prediction performance for test set A in green. For this test, four capacity series over 7920 hours from the same storage conditions of training series are predicted and analyzed through using both Model 1 and Model 2, while the corresponding future capacity prediction results are illustrated in Fig. 8.

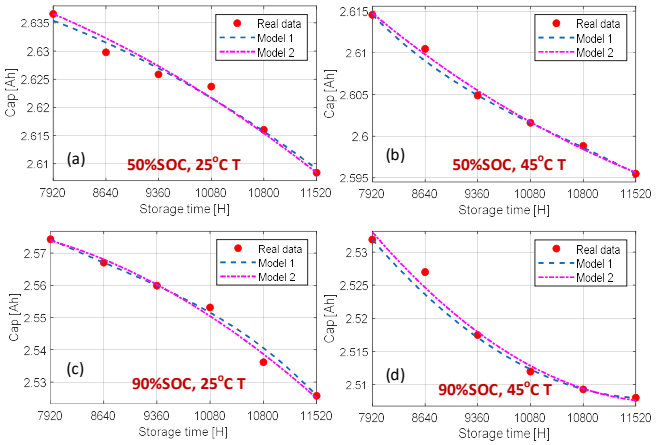

Fig. 8. Future capacity prediction results for cells under different storage cases of test set A: a) Test 1 set, b) Test 2 set, c) Test 3 set, b) Test 4 set.

TABLE III
EVALUATION METRICS FOR CASE STUDY OF TEST SET A

Test set	Model 1			Model 2		
	MAE [Ah]	**RMSE [Ah]**	R^2	**MAE [Ah]**	**RSME [Ah]**	R^2
Test 1(A)	0.003	0.0013	0.98	0.003	0.0012	0.98
Test 2(A)	0.003	0.0011	0.98	0.002	0.0008	0.99
Test 3(A)	0.004	0.0023	0.98	0.003	0.0019	0.99
Test 4(A)	0.005	0.0026	0.97	0.003	0.0022	0.98

From Fig. 8, the predicted capacity points from two models well match the overall trends of real capacity series for all four cases, indicating that satisfactory extrapolated prediction could be achieved by using both Model 1 and Model 2. According to the corresponding evaluation metrics illustrated in Table III, the largest RMSEs are achieved for Test 4(A) set with 0.0026Ah for Model 1 and 0.0022Ah for Model 2, respectively. These values are 136.4% and 175.0% larger than those from Test 2(A) set (the most accurate one). However, the R^2 values of all these test cases are still larger than 0.97, implying that the base model part of the designed transferred RNN framework could offer reliable extrapolated prediction performance of future calendar capacities under the same witnessed conditions.

C. Case study for test set B

After well training the base model part by using battery accelerated calendar capacity degradation data under both high SOC and temperature levels, this case study focuses on the

adjustment of transfer model part and the performance evaluation of battery health prognostics under unwitnessed storage cases in purple. Specifically, a small portion (20%) of starting capacity data before 2160 hours from capacity series of test set B (Test 1(B), 2(B),…,5(B)) is utilized to optimize the transfer model part of transferred RNN framework. Then the well-tuned transferred RNN model is adopted to predict future capacity points of interest from these unwitnessed storage conditions.

Fig. 9 illustrates the future capacity prediction results of two test series under the same SOC of 20% but different storage temperature levels (25℃ and 45℃). Through using 20% portion starting data to tune transfer model part, both Model 1 and Model 2 are able to provide satisfactory ageing prognostic performance for these two cases. According to the related evaluation metrics in Table IV, the R^2 values are larger than 0.96. The RSMEs of Model 2 are 0.0069Ah for Test 1(B) and 0.0072Ah for Test 2(B), which is 8.0% and 6.5% smaller than those from Model 1. Therefore, through involving two additional terms to reflect impact factors of storage SOC and temperature, Model 2 presents a slightly better prediction accuracy than Model 1 for 20% SOC cases.

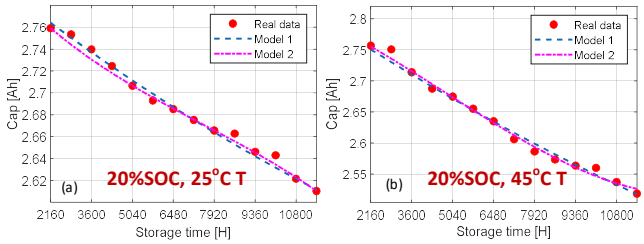

Fig. 9. Future capacity prediction results for cells of test set B under 20% SOC cases: a) 25℃ temperature (Test 1), b) 45℃ temperature (Test 2).

Next, we focus on the future capacity predictions under the same temperature of 10℃ but different storage SOC levels (50% and 90%). According to the prediction results shown in Fig. 10, after using 20% starting portion data of these two capacity series to optimize transfer model part, the predictions from both Model 1 and Model 2 could also well match the overall trend of real capacity series. However, Model 2 presents better prediction results than Model 1 especially for Test 4(B) case. Quantitatively, the R^2 values of Model 1 are both 0.95 for these two cases, while it becomes over 0.97 for Model 2. The worst RMSE of 0.0089Ah is obtained for Model 1 in Test 4(B) case. This can be explained as the difference between the predicted and the real capacity values increases obviously after 9360 hours. Therefore, for the same storage temperature but different SOC conditions, Model 2 also provides better prediction results than Model 1.

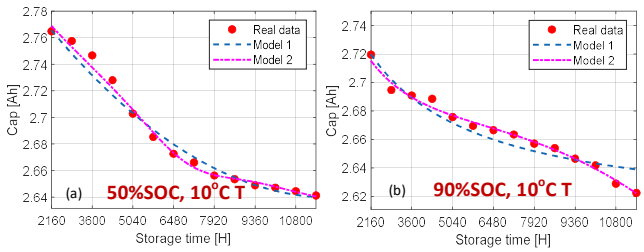

Fig. 10. Future capacity prediction results for cells of test set B under 10℃ temperature cases: a) 50% SOC (Test 3), b) 90% SOC (Test 4).

Finally, a test using the derived transferred RNN framework to predict future capacity points under a totally new storage condition with 20% SOC and 10℃ temperature is carried out. Fig. 11 illustrates the future capacity prediction results of both Model 1 and Model 2 for such case. Interestingly, it is clear that Model 1 with simple structure cannot well capture the real future capacities all the time. Its prediction performance is acceptable before 3600 hours but afterwards, large mismatches happen. Quantitatively, the MAE, RMSE and R^2 here are 0.029Ah, 0.0096Ah and 0.93, respectively. In comparison, Model 2 is still able to present satisfactory future capacity prediction results. Here the MAE, RMSE and R^2 are 0.012Ah, 0.0069Ah and 0.98, which are 58.6%, 28.1% and 5.4% better than those of Model 1, respectively. In conclusion, through adding two additional terms to consider the impact factors of storage SOC and temperature, Model 2 is capable of generalizing better than Model 1. Such superiority becomes apparent for the unwitnessed case that both battery storage SOC and temperature are different from those of training case (accelerated capacity degradation series).

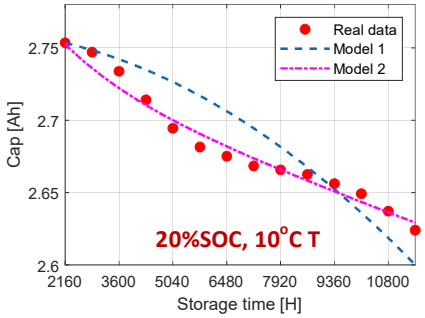

Fig. 11. Future capacity prediction results for cell of test set B under 20% SOC and 10 ℃ temperature storage case (Test 5).

TABLE IV
EVALUATION METRICS FOR CASE STUDY OF TEST SET B

Test set	Model 1			Model 2		
	MAE [Ah]	**RMSE [Ah]**	R^2	**MAE [Ah]**	**RSME [Ah]**	R^2
Test 1(B)	0.025	0.0075	0.96	0.021	0.0069	0.98
Test 2(B)	0.028	0.0077	0.97	0.027	0.0072	0.98
Test 3(B)	0.018	0.0085	0.95	0.010	0.0076	0.97
Test 4(B)	0.021	0.0089	0.95	0.008	0.0064	0.98
Test 5(B)	0.029	0.0096	0.93	0.012	0.0069	0.98

D. Comparisons and discussions

In this subsection, to further explore the performance of derived transferred RNN for battery future calendar capacity ageing prognostics, another two typical feedforward neural networks (NN) including the backpropagation (BP)-based NN and radial basis function (RBF)-based NN are also enhanced with the transfer part and compared under the same calendar capacity sets. Specifically, after using the same logic mentioned in Subsection III-B to add the transfer part, the transferred BP-NN and transferred RBF-NN are derived. Then the base model parts of these two NNs are also trained by the same accelerated capacity data in blue and tested under both witnessed cases (test set A) and unwitnessed cases (test set B). Without the loss of

generality, the structure of Model 2 with four input terms is utilized for all three NNs of interest.

1) Comparison under witnessed storage cases: To explore and evaluate each NN model's calendar degradation prognostics performance under the same storage conditions as the training series, the evaluation metrics (MAE, RMSE and R^2) for transferred RNN, BP-NN and RBF-NN in terms of prediction results of Test 4(A) (the worst case for RNN) are illustrated in Fig. 12. Through using the Matlab 2020 with a 2.40 GHz Intel Pentium 4 CPU, BP-NN achieves the smallest training time with 10.3s, while RBF-NN provides the longest time with 14.6s, which is 23% larger than that of RNN. This is reasonable as RBF-NN has a more complicated function within its neurons. However, all training time is still within 15s, indicating that the acceptable computational burden can be obtained for all these three NNs. It can be seen that for the future calendar capacity predictions under the same storage conditions, all these three NN models could provide competitive performance as their R^2 values are larger than 0.95. In comparison, the transferred RNN achieves the best results, whose RMSE is 24.1% and 40.5% smaller than that from BP-NN and RBF-NN, respectively.

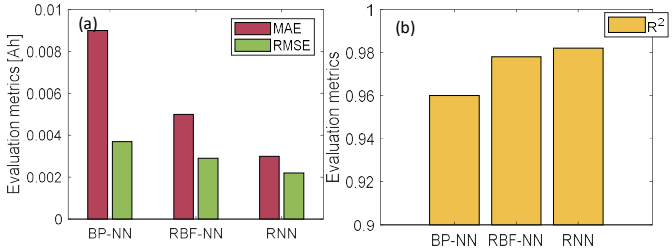

Fig. 12. Evaluation metrics of using different models for Test 4(A): a) MAE and RMSE, b) R^2 value.

2) Comparison under unwitnessed storage cases: For the sake of exploring each NN model's calendar degradation prognostics performance under the storage conditions that are different from the training series, the corresponding evaluation metrics for Test 5(B) (the worst case for RNN) are compared and illustrated in Fig. 13. The optimization processes of transfer part in these three transferred NNs can be completed within 4s, further indicating the effectiveness of derived transfer framework. Due to the storage SOC and temperature of Test 5(B) case being totally different from the training series, it is expected that MAE, RMSE and R^2 values are all worse than those of witnessed storage cases. Quantitatively, the MAE, RMSE and R^2 of transferred RBF-NN are 19.0%, 7.5% and 1.1% better than those of transferred BP-NN (the worst one). In contrast, by involving the recurrent link within the NN structure, transferred RNN achieves the obvious improvements for time-series future capacity predictions. In this case, MAE is 52% decreased, RMSE is 25.8% decreased, and R^2 is 4.3% increased, indicating the superiorities of coupling recurrent links for time-series future calendar capacity health prognostics under unwitnessed storage cases.

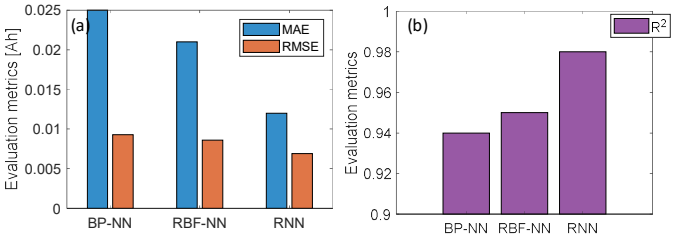

Fig. 13. Evaluation metrics of using different models for Test 5(B): a) MAE and RMSE, b) R^2 value.

3) Further discussions: As the obvious battery capacity degradation would take several months or years under storage conditions, while the computational burden of developed model is in the second level. In this context, the transferred RNN-based model designed in this study is practical to be implemented in real-time applications. In general, for battery health prognostics, the smaller prediction error a designed method can achieve, the better prediction results this method can provide. However, this acceptable error rate would be changed based on different requirements in both energy and transportation applications. For example, engineers from some vehicle companies suggest it to be within 3%, while some energy storage companies suggest it to be within 5% to our best knowledge. Considering battery health status plays a vital role in affecting battery performance and safety, less acceptable error rate is worth exploring to widen energy-transportation applications. As the proposed transferred RNN approach presents the superiorities in terms of data-driven nature, flexibility and free of battery ageing mechanism, when the relevant data from other types of batteries are available, it can be extended to perform calendar health prognostics for these batteries.

In addition, note that battery capacity would not usually degrade over 15% or 20% during storage cases particular for EV applications [6], this study mainly focuses on the battery calendar ageing prognostics under the relatively low capacity loss, which is required by the vehicle companies. Although generating such battery calendar capacity loss data has spent a long experimental time over one year, our future work would focus on continue generating longer-term battery calendar ageing data under storage conditions, thus benefitting calendar health prognostics with high capacity loss for battery second-life applications.

V. CONCLUSION

Battery-based energy storage system plays a vital role in promoting the low carbon industrial and social economy of energy-transportation nexus. In this study, an effective data-driven framework that derives the novel transferred RNN to the calendar ageing prognostics of Li-ion battery under various storage cases is proposed to benefit the health managements of battery-based energy storage system. The transferred RNN-based framework contains two parts: base model part as well as transfer model part. The base model part is trained by using the time-saving and easily-collected accelerated ageing dataset, while the transfer model part is tuned by using only a small starting portion of capacity series of interest, bringing the benefits to significantly reduce the required ageing experiment

burden. Illustrative study shows that the proposed framework is reliable and generalizes well for future capacity ageing prognostics under both witnessed and unwitnessed conditions. It is also confirmed that Model 2 containing the additional terms of impact SOC and temperature factors could provide better prediction accuracy and generalization ability especially for the storage case that is totally different from training series. Though using only 20% starting portion data to tune the transfer part of the transferred RNN-based framework, satisfactory prediction accuracy with R^2 over 0.97 could be obtained for such type of model. Considering the significant time-consumption for long-term battery ageing experiments, the proposed transferred RNN-based framework provides a promising way to perform effective future calendar ageing prognostics using only a small portion of the capacity series of interest. After collecting suitable portion ageing data of battery, engineers could use this framework to predict and get useful information of future capacity series under unwitnessed storage conditions, further benefitting health and life-cycle cost analysis of battery-based energy storage systems for better energy and transportation applications.

REFERENCE

[1] X. Yuan, L. Li, H. Gou, and T. Dong. "Energy and environmental impact of battery electric vehicle range in China." Applied Energy 157 (2015): 75-84.

[2] Z. Wei, H. He, J. Pou, K. L. Tsui, Z. Quan, and Y. Li. "Signal-disturbance interfacing elimination for unbiased model parameter identification of lithium-ion battery." IEEE Transactions on Industrial Informatics (2020).

[3] X. Sui, S. He, S. B. Vilsen, J. Meng, R. Teodorescu, and D. I. Stroe. "A review of non-probabilistic machine learning-based state of health estimation techniques for lithium-ion battery." Applied Energy 300 (2021): 117346.

[4] Y. Wang, J. Tian, Z. Sun, L. Wang, R. Xu, M. Li, and Z. Chen. "A comprehensive review of battery modeling and state estimation approaches for advanced battery management systems." Renewable and Sustainable Energy Reviews 131 (2020): 110015.

[5] K. Liu, Y. Li, X. Hu, M. Lucu, and W. D. Widanage. "Gaussian process regression with automatic relevance determination kernel for calendar aging prediction of lithium-ion batteries." IEEE Transactions on Industrial Informatics 16, no. 6 (2019): 3767-3777.

[6] T. R. Ashwin, A. Barai, K. Uddin, L. Somerville, A. McGordon, and J. Marco. "Prediction of battery storage ageing and solid electrolyte interphase property estimation using an electrochemical model." Journal of Power Sources 385 (2018): 141-147.

[7] J. de Hoog, J. M. Timmermans, D. Ioan-Stroe, M. Swierczynski, J. Jaguemont, S. Goutam, N. Omar, J. V. Mierlo, and P. V. D. Bossche. "Combined cycling and calendar capacity fade modeling of a Nickel-Manganese-Cobalt Oxide Cell with real-life profile validation." Applied Energy 200 (2017): 47-61.

[8] S. L. Hahn, M. Storch, R. Swaminathan, B. Obry, J. Bandlow, and K. P. Birke. "Quantitative validation of calendar aging models for lithium-ion batteries." Journal of Power Sources 400 (2018): 402-414.

[9] Y. Gao, X. Zhang, B. Guo, C. Zhu, J. Wiedemann, L. Wang, and J. Cao. "Health-aware multiobjective optimal charging strategy with coupled electrochemical-thermal-aging model for lithium-ion battery." IEEE Transactions on Industrial Informatics 16, no. 5 (2019): 3417-3429.

[10] J. Hu, Q. Sun, Z. S. Ye, and Q. Zhou. "Joint modeling of degradation and lifetime data for RUL prediction of deteriorating products." IEEE Transactions on Industrial Informatics 17, no. 7 (2020): 4521-4531.

[11] Z. Lyu, G. Wang, and R. Gao. "Li-ion battery prognostic and health management through an indirect hybrid model." Journal of Energy Storage 42 (2021): 102990.

[12] R. R. Richardson, C. R. Birkl, M. A. Osborne, and D. A. Howey. "Gaussian process regression for in situ capacity estimation of lithium-ion batteries." IEEE Transactions on Industrial Informatics 15, no. 1 (2018): 127-138.

[13] H. T. Lin, T. J. Liang, and S. M. Chen. "Estimation of battery state of health using probabilistic neural network." IEEE transactions on industrial informatics 9, no. 2 (2012): 679-685.

[14] C. She, Z. Wang, F. Sun, P. Liu, and L. Zhang. "Battery aging assessment for real-world electric buses based on incremental capacity analysis and radial basis function neural network." IEEE Transactions on Industrial Informatics 16, no. 5 (2019): 3345-3354.

[15] G. Ma, Y. Zhang, C. Cheng, B. Zhou, P. Hu, and Y. Yuan. "Remaining useful life prediction of lithium-ion batteries based on false nearest neighbors and a hybrid neural network." Applied Energy 253 (2019): 113626.

[16] G. Dong, F. Yang, Z. Wei, J. Wei, and K. L. Tsui. "Data-driven battery health prognosis using adaptive Brownian motion model." IEEE Transactions on Industrial Informatics 16, no. 7 (2019): 4736-4746.

[17] X. Hu, L. Xu, X. Lin, M. Pecht. "Battery lifetime prognostics." Joule 4, no. 2 (2020): 310-346.

[18] L. Ren, J. Dong, X. Wang, Z. Meng, L. Zhao, and M. J. Deen. "A data-driven auto-cnn-lstm prediction model for lithium-ion battery remaining useful life." IEEE Transactions on Industrial Informatics 17, no. 5 (2020): 3478-3487.

[19] Y. Tan, and G. Zhao. "Transfer learning with long short-term memory network for state-of-health prediction of lithium-ion batteries." IEEE Transactions on Industrial Electronics 67, no. 10 (2019): 8723-8731.

[20] G. W. You, S. Park, and D. Oh. "Diagnosis of electric vehicle batteries using recurrent neural networks." IEEE Transactions on Industrial Electronics 64, no. 6 (2017): 4885-4893.

[21] Y. Zhang, R. Xiong, H. He, and M. G. Pecht. "Long short-term memory recurrent neural network for remaining useful life prediction of lithium-ion batteries." IEEE Transactions on Vehicular Technology 67, no. 7 (2018): 5695-5705.

[22] K. Liu, Y. Shang, Q. Ouyang, and W. D. Widanage. "A data-driven approach with uncertainty quantification for predicting future capacities and remaining useful life of lithium-ion battery." IEEE Transactions on Industrial Electronics 68, no. 4 (2020): 3170-3180.

[23] M. Dubarry, N. Qin, and P. Brooker. "Calendar aging of commercial Li-ion cells of different chemistries–A review." Current Opinion in Electrochemistry 9 (2018): 106-113.

[24] V. Sulzer, P. Mohtat, A. Aitio, S. Lee, Y. T. Yeh, F. Steinbacher, M. U. Khan et al. "The challenge and opportunity of battery lifetime prediction from field data." Joule (2021).

[25] M. Lewerenz, G. Fuchs, L. Becker, and D. U. Sauer. "Irreversible calendar aging and quantification of the reversible capacity loss caused by anode overhang." Journal of Energy Storage 18 (2018): 149-159.

[26] A. Eddahech, O. Briat, and J. M. Vinassa. "Performance comparison of four lithium–ion battery technologies under calendar aging." Energy 84 (2015): 542-550.

[27] B. Zraibi, C. Okar, H. Chaoui, and M. Mansouri. "Remaining Useful Life Assessment for Lithium-Ion Batteries Using CNN-LSTM-DNN Hybrid Method." IEEE Transactions on Vehicular Technology 70, no. 5 (2021): 4252-4261.

[28] I. Goodfellow, Y. Bengio, and A. Courville. "Machine learning basics." Deep learning 1 (2016): 98-164.

[29] F. Zhuang, Z. Qi, K. Duan, D. Xi, Y. Zhu, H. Zhu, H. Xiong, and Q. He. "A comprehensive survey on transfer learning." Proceedings of the IEEE 109, no. 1 (2020): 43-76.

[30] R. Pascanu, T. Mikolov, and Y. Bengio. "On the difficulty of training recurrent neural networks." In International conference on machine learning, pp. 1310-1318. PMLR, 2013.

Kailong Liu (M'18) received the Ph.D. degree in electrical engineering from Queen's University Belfast, United Kingdom in 2018. He is an Assistant Professor in the Warwick Manufacturing Group, University of Warwick, United Kingdom. His research interests include modeling, optimization and control with applications to electrical/hybrid vehicles, energy storage, battery manufacture and management. Dr. Liu is on editorial boards of some journals of his area including Renewable and Sustainable Energy Reviews, IEEE/CAA Journal of Automatica Sinica, Control Engineering Practice.

Qiao Peng is a PhD candidate at Queen's University Belfast, UK. She obtained the BSc degree at Nanjing University of Information Science & Technology, China and the MSc degree at Queen's University Belfast, in 2016 and 2017, respectively. Her research interests include the applications of machine learning, data analysis, modelling and prediction technologies in many fields such as battery management, and credit union performance assessment.

Minrui Fei is the professor of the School of Mechatronic Engineering and Automation, Shanghai University, Deputy Director of the Academic Committee of Shanghai University, Head of the 111 Intelligence Introduction Base of the Department of Intelligent Measurement and Control and Application of Complex Networked Systems of the Ministry of Science and Technology / Ministry of Education, Director of the Shanghai Key Laboratory of Power Station Automation Technology, Shanghai Intelligence Project leader of the International Joint Laboratory of Automation and Networked Control, Fellow of ASIASIM Federation, Fellow of China Simulation Society, Honorary Vice Chairman (Fifth and Sixth Vice Chairman) and Director of Life System Modeling and Simulation Committee, Editor of "Journal of System Simulation" Committee. He engaged in intelligent networked control theory, system and simulation research, where he presided over 30 vertical topics such as national key research and development projects, national natural science fund key projects, and national major instrument special projects. He published more than 140 SCI papers in IEEE and IFAC, 3 academic books, 11 Springer book chapters and obtained more than 100 intellectual property rights. He won the second prize of National Science and Technology Progress Award, the first prize of Shanghai Science and Technology Progress Award, the first prize of China Machinery Industry Science and Technology Award, and the first prize of Natural Science of China Simulation Society.

Hongbin Sun (Fellow, IEEE) received the double B.S. degrees from Tsinghua University, Beijing, China, in 1992 and the Ph.D. degreefrom the Department of Electrical Engineering, Tsinghua University, in 1996. From September 2007 to September 2008, he was a Visiting Professor with the School of Electrical Engineering and Computer Science, Washington State University, Pullman, WA, USA. He is currently a ChangJiang Scholar Chair Professor with the Department of Electrical Engineering and the Director of Energy Management and Control Research Center, Tsinghua University. He has authored or coauthored more than 400 peer-reviewed papers, within which more than 60 are IEEE and IET journal papers, and four books. He has been granted five U.S. Patents of Invention and more than 100 Chinese Patents of Invention. His research interests include electric power system operation and control with specific interests on energy management system, system-wide automatic voltage control, and energy system integration. He is currently an IET Fellow. He is also the Editor of the IEEE Transactions on Smart Grid, an Associate Editor for the IET Renewable Power Generation, and a Member of the Editorial Board of four international journals and several Chinese journals.

Huimin Ma (M, IEEE) was the Director of the 3D Imaging Lab, Department of Electronic Engineering, Tsinghua University. She is currently a Professor with the School of Computer and Communication, University of Science and Technology. She is also the Dean of the Department of Internet of Things and Electronic Engineering and the Vice President of the Institute of Artificial Intelligence. She introduces semantic prior of cognition and psychology into machine learning, and studies object detection, cognition and navigation in complex scenes. In recent years, her researches were published in the high level journals (TPAMI and TIP) and the international conferences (CVPR and NIPS). Her research interest is 3-D image cognition and simulation. She is also the Secretary-General of the China Society of Image and Graphics.

Tianyu Hu (M'17) received the Ph.D. degree from Tsinghua-Berkeley Shenzhen Institute, Tsinghua University, China, in 2020. He joined the School of Computer and Communication Engineering, University of Science and Technology Beijing in September 2020 as an associate professor. His research interests include deep learning, logic, and cognition decision.